Structural Engineering and Mechanics, Vol. 12, No. 2 (2001) 169-188 169
DOI: http://dx.doi.org/10.12989/sem.2001.12.2.169

Mechanical behaviour of a syntactic foam/glass fibre composite sandwich: experimental results*

Enrico Papa[1] and Alberto Corigliano[1]

Dipartimento di Ingegneria Strutturale, Facoltà di Ingegneria Leonardo, Politecnico di Milano, Piazza Leonardo da Vinci 32, I-20133 Milano, Italy

Egidio Rizzi[1]

Dipartimento di Ingegneria Civile e Ambientale, Facoltà di Ingegneria di Taranto, Politecnico di Bari, Via Orabona 4, I-70125 Bari, Italy

Abstract. This note presents the main results of an experimental investigation into the mechanical behaviour of a composite sandwich conceived as a lightweight material for naval engineering applications. The sandwich structure is formed by a three-dimensional glass fibre/polymer matrix fabric with transverse piles interconnecting the skins; the core is filled with a polymer matrix/glass microspheres syntactic foam; additional Glass Fibre Reinforced Plastics extra-skins are laminated on the external facings of the filled fabric. The main features of the experimental tests on syntactic foam, skins and sandwich panels are presented and discussed, with focus on both in-plane and out-of-plane responses. This work is part of a broader research investigation aimed at a complete characterisation, both experimental and numerical, of the complex mechanical behaviour of this composite sandwich.

Key words: mechanical tests; syntactic foam; glass fibre; composite sandwich.

1. Introduction

This paper presents an experimental study on the mechanical behaviour of a syntactic foam/glass fibre composite sandwich. The external facings of the sandwich (*skins*) are made of glass fibre/polymer matrix composites, whereas the central part of the sandwich (*core*) consists of a syntactic foam made with an epoxy resin matrix embedding randomly-dispersed hollow glass microspheres. In order to reduce the risk of delamination, the core is crossed by several piles that interconnect the interior layers of the upper and lower skins in a true three-dimensional fabric (see Fig. 1). The main potential weakness of this composite typology lies in fact in the possible decohesion at the interface between skins and core, which possess considerably different mechanical properties: the skins must be stiff and strong, while the core should mainly display a low specific weight, together with a sufficiently-enough shear stiffness. Glass Fibre Reinforced Plastics (GFRP) extra-skins are further laminated on the external facings of the sandwich to improve its bending performance. Light sandwiches of the kind considered here are particularly appropriate for naval engineering

[1] Associate Professor
**Dedicated to Prof. Giulio Maier on the occasion of his 70th birthday!*

applications, since they present a low specific weight combined with considerable stiffness and strength (see e.g. Kuenzi 1965, Plantema 1966, Allen 1969, Smith 1990, Hull and Clyne 1996).

For the analysis and design of structural elements built with this heterogeneous material, both the mechanical behaviour of the single sandwich components (syntactic foam, skins, extra-skins) and the global response of the assembled sandwich elements must be assessed. Accordingly, an experimental programme has been carried out at the Department of Structural Engineering, Politecnico di Milano. Particular attention has been devoted to both the in-plane and the out-of-plane behaviour. Uniaxial and biaxial tension/compression tests on sandwich components and sandwich panels have been performed; three and four point bending tests have been carried out on syntactic foam specimens and sandwich panels. The experimental results have been also simulated numerically by separate Finite Elements analyses through suitable engineering-oriented computational procedures, developed for both the syntactic foam (Rizzi *et al.* 2000) and the whole sandwich (Corigliano *et al*. 2000).

The paper is organised as follows: in Section 2 the sandwich structure and its components are briefly described. Section 3 reports the experimental results obtained for the syntactic foam, while Section 4 the results attained for the sandwich extra-skins and for the composite sandwich specimens. Finally, Section 5 collects some closing remarks and draws some possible future perspectives of the present study.

2. The syntactic foam/glass fibre composite sandwich

The syntactic foam/glass fibre composite sandwich was manufactured by a former branch of Intermarine S.p.A. (Italy). The sandwich structure is depicted in Fig. 1. The core is built starting from a sandwich-fabric produced by Parabeam (The Netherlands), which was deeply studied in the framework of a Brite Euram project (Aficoss-Advanced Fabric for Integrally-woven Composite Sandwich Structures, see van Vuure 1997, van Vuure *et al.* 2000). Two plane-weave are maintained, through pre-impregnation, at a fixed distance by interwoven threads called piles (Fig. 1b). Then the core is filled with a syntactic foam manufactured by the same industry which furnished the whole sandwich panels. The syntactic foam, named Tencara 2000^{TM}, is obtained by embedding hollow air-filled glass microspheres into a SP Ampreg 20^{TM} epoxy resin treated with SP Ampreg Ultraslow^{TM} hardener. The air-filled hollow glass microspheres are 3M Scotchlite^{TM} Glass Bubbles, type K1, with average diameter of 70 μm and average wall thickness of 0.58 μm. These microspheres are made with a borosilicate glass, water resistant and chemically stable. The specific weight of the resulting syntactic foam is about 0.55 g_f/cm^3. General information about uses and applications of syntactic foams, their mechanical properties and manufacturing procedures may be found in Rizzi *et al*. (2000) and references quoted therein; specific details concerning the manufacturing procedure of this syntactic foam are available in (Palumbo *et al.* 1996, Palumbo and Tempesti 1997, 1998, Rizzi *et al.* 2000).

Two extra-skins of ROVIMAT 1200^{TM} (made of glass-fibres and polymer matrix) are laminated on the 3D fabric facings in order to improve the mechanical performances under bending. Each extra-skin is composed by a non-directional GFRP fabric, called MAT 300^{TM}, and by a plane weave GFRP fabric, called ROVING 900^{TM}, obtained by sewing two plane-weave tissues. The ROVIMAT 1200^{TM} extra-skin has a thickness of 2.5 mm, while the global thickness of the sandwich is 15 mm.

It is worth-noting that, due to an incorrect manufacturing procedure, the set of sandwich panels

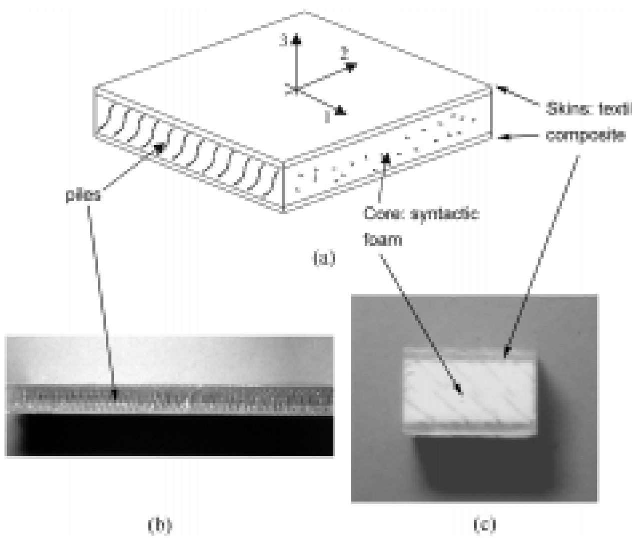

Fig. 1 The composite sandwich under study: (a) overall schematic view; (b) glass fibre/polymer matrix fabric with piles interconnecting the skins; (c) syntactic foam core

provided by the manufacturer for the testing campaign presented the piles not completely stretched along the vertical direction but rather inclined at about 45°: this fact obviously affected the mechanical properties, as observed from the experimental results reported in Section 4.

3. Experimental tests on the syntactic foam

The mechanical behaviour of the Tencara 2000™ syntactic foam has been investigated through the following series of tests on specimens directly prepared by the manufacturer: uniaxial compression, uniaxial tension, pure torsion, biaxial compression and three point bending tests on notched specimens. For each group of tests, specimen shapes and sizes have been chosen according to the relevant standards and compatibly with the capabilities and requirements of the available testing devices (load-carrying capacity, end grips dimensions, etc.): an Instron 8652 machine, an MTS 329.10 S machine and a biaxial fatigue testing device, designed by Prof. Maier and Nappi and developed at the Department of Structural Engineering (Papa and Nappi 1995).

3.1 Uniaxial compression tests on the syntactic foam

The uniaxial compression tests were performed on the MTS 329.10 S machine, according to the ASTM D 695 standard for composite materials. The main difficulty in performing these kinds of tests is represented by friction at the interface between specimen and loading platens. To reduce friction confinement, the ASTM suggests particular specimen shapes with specific size ranges: the specimens should be circular cylinders with height to diameter ratio greater than or equal to 1.5. Accordingly, cylindrical syntactic foam specimens were designed with a 30 mm diameter and a 75 mm height (see Fig. 2a). Furthermore, friction effects were reduced by interposing two Teflon sheets between specimen and loading platens. The longitudinal and circumferential strains were measured

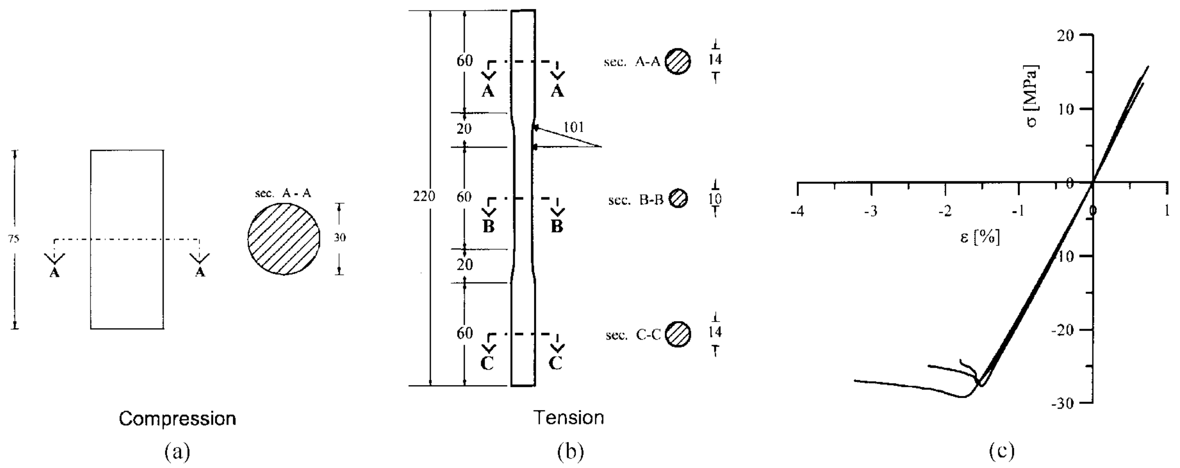

Fig. 2 Uniaxial tension/compression tests on the syntactic foam: specimen geometry (dimensions in mm) for (a) compression and (b) tension specimens; (c) stress-strain curves of tests II.1-II.3 (Table 1) and IV.1-IV.3 (Table 3)

by electric strain gauges directly glued onto the specimens. To capture the post-peak behaviour of the material, the tests were driven under displacement control, with different constant cross-head velocities varying between 0.05 to 5.00 mm/min.

Table 1 reports the salient mechanical data obtained from the tests: Young's modulus E, Poisson's ratio ν, maximum compressive strength (σ_{peak}) and corresponding strain (ε_{peak}). It is worth-mentioning that the stiffness shown by specimens I.1-I.4 is lower than that of tests II.1-II.5. Indeed, the producer provided two separate sets of specimens: the second set (II.1-II.5) showed a considerably lower presence of voids with respect to the first set (I.1-I.4). This explains the larger stiffness (about 10% higher) of the second specimens. Into each group of specimens the recorded data were relatively low scattered and practically independent of the imposed cross-head velocities.

The stress-strain curves for all the specimens of Table 1 are practically linear up to the stress peak. After peak, the curves show softening branches of different steepness and length which generally tend to reach a constant level of residual strength. In Fig. 2c the stress-strain plots for specimens II.1-II.3 are shown.

To investigate possible effects of progressive elastic stiffness degradation (elastic-damage), three additional compression tests were also performed by considering repeated full unloading/reloading paths at regular intervals of strain increase (about each 1% strain) in the non-linear range: the elastic modulus in the unloading/reloading branches of the stress-strain curves turned out to remain practically constant and equal to the initial value, so that elastic-damage did not appear to be a significant mechanical feature of the foam behaviour in compression. However, this aspect has not been further investigated in the uniaxial tension tests since, as it will be shown in Section 3.2, failure occurs rather abruptly at peak stress in a very brittle way. Thus, further tests should be performed to draw more definite conclusions about elastic stiffness degradation of the syntactic foam.

Failure under compression is induced by strain localization along a shear band inclined at an angle of about 45° with respect to the loading axis. During failure, the specimen is separated in two parts that slide with respect to each other. The residual strength observed in the stress-strain curve depends on the interlocking and friction phenomena which govern sliding after the onset of strain

Table 1 Experimental data of uniaxial compression tests on the syntactic foam manufactured by the producer

Test number	Specific weight γ (g_f/cm^3)	Test velocity (mm/min)	E (MPa)	ν	σ_{peak} (MPa)	ε_{peak} (%)
I.1	0.535	0.05	1578	0.365	26.87	2.55
I.2	0.515	0.50	1589	–	28.96	2.29
I.3	0.535	0.50	1638	0.329	29.32	2.00
I.4	0.535	0.50	1641	–	28.04	2.83
II.1	0.551	0.05	1858	0.355	27.78	1.51
II.2	0.562	0.50	1870	0.318	30.88	1.61
II.3	0.539	0.50	1838	0.320	28.28	1.63
II.4	0.548	0.50	1838	0.314	27.30	1.57
II.5	0.549	5.00	1773	0.305	29.23	1.76

localization. This collapse mechanism resembles in fact the failure mode observed in many granular materials such as e.g. dense sands subjected to triaxial compression. This analogy should be due to the crushing of the hollow glass microspheres, which simultaneously loose also contact with the surrounding epoxy resin matrix. It is important to note that several glass microspheres may already fail during the preparation phase of the syntactic foam.

Table 2 shows the results obtained on two additional specimens (III.1, III.2) manufactured at the Department of Chemistry and Physics of Materials, University of Brescia. These specimens were made with the same epoxy resin but the matrix was filled with different hollow glass microspheres (called K37), which are heavier than the K1 bubbles (0.37 g_f/cm^3 vs. 0.125 g_f/cm^3) and present a smaller average diameter (50 μm vs. 70 μm) and a larger wall thickness (1.28 μm vs. 0.58 μm). Consequently, they are less prone to fail during the preparation phase of the syntactic foam. Furthermore, while specimen III.1 was prepared with plain glass microspheres K37 as provided by the manufacturer, the microspheres used for specimen III.2 were previously winnowed with sieves having diameters varying between 32 and 45 μm. Moreover, a different production technique was used at the University of Brescia, which allowed to eliminate almost completely the voids into the syntactic foam and to push the volumetric fraction of the microspheres up to the high value of 75%. Table 2 (vs. Table 1) shows the considerable increase of strength (around two and a half times) and stiffness (almost two times) for specimens III.1-III.2 with respect to series I and II. This result agrees well with the conjecture that the mechanical properties should be substantially affected by the percentage of glass microspheres with smaller diameter. It is worth-noting that the significant increase of strength and stiffness is gained without a corresponding considerable increase of specific weight, which grows approximately only by 10% (from about 0.55 g_f/cm^3 to about 0.60 g_f/cm^3). Lateral strains (so Poisson's ratio ν) were not measured for these two tests.

3.2 Uniaxial tension tests on the syntactic foam

The uniaxial tension tests were made on the MTS 329.10 S machine. Specimens shape and size were determined according to the ASTM D 638 for composite materials. This code recommends flat *dog-bone-shaped* specimens with suitable ranges of dimensions. Due to ease of workability by the manufacturer, the specimens used were instead circular cylindrical bars with tapered cross sections (Fig. 2b), as usually recommended by steel standards. The longitudinal and circumferential strains were measured by electric strain gauges directly glued onto the specimens.

Table 2 Experimental data of uniaxial compression tests on the syntactic foam manufactured at the University of Brescia, Dept. of Chemistry and Physics of Materials

Test number	Specific weight γ (g_f/cm^3)	Test velocity (mm/min)	E (MPa)	σ_{peak} (MPa)	ε_{peak} (%)
III.1	0.62	0.5	3145	72.93	2.86
III.2	0.62	0.5	3693	77.47	2.70

Table 3 Experimental data of uniaxial tension tests on the syntactic foam manufactured by the producer

Test number	Specific weight γ (g_f/cm^3)	Test velocity (mm/min)	E (MPa)	ν	σ_{peak} (MPa)	ε_{peak} (%)
IV.1	0.55	0.05	2009	0.354	13.43	0.68
IV.2	0.55	0.50	2240	0.340	14.09	0.64
IV.3	0.55	0.50	2196	0.320	15.63	0.75

Three tests were performed, with results reported in Table 3. Some scatter in elastic parameters, peak stresses and strains can be noticed. The maximum difference in strength (of about 10%) depends on the failure mode: only the specimen with higher strength value broke correctly in its central part (σ_{peak}=15.63 MPa, ε_{peak}=0.75%), while the other two tests registered breakage in zones near the tapered cross sections, owing probably to the presence of microdefects induced by the preparation phase.

The stress-strain curves of all the specimens show a linear elastic behaviour until a perfectly brittle failure (Fig. 2c). Actually, right before sudden rupture, the curves bend a little from linearity due to the microcracking developing between matrix and spheres.

The average value of elastic modulus is around $E_t = 2200$ MPa, which is about 20% greater than the average Young's modulus in compression $E_c = 1850$ MPa, for the specimen belonging to the second set (Table 1), to which belonged also the tensile specimens. This difference in elastic stiffness in tension and compression may be due to the presence of air bubbles between matrix and filler. The average value of Poisson's ratio (about 0.34) is instead practically identical to the mean value obtained for the compression tests.

3.3 Torsion tests on the syntactic foam

The torsion tests were also carried out on the MTS 329.10S testing device. Since it was not possible to recover ASTM standards specifically referred to torsion tests, the specimens used were identical to those of the tension tests. Three tests were performed, but one of them gave unreliable results owing to a premature failure near the end-grip zone.

The behaviour of the syntactic foam is almost perfectly brittle (see Fig. 3): the average value of the maximum shear stress at rupture is equal to 14.77 MPa. The average value of shear modulus (about 780 MPa) is quite in agreement with a shear modulus evaluated with the classical formula for isotropic linear elastic materials, by taking the tensile stiffness $E_t = 2200$ MPa as Young's modulus and $\nu = 0.34$ as Poisson's ratio. This fact seems to support the conjecture that the tensile Young's modulus would be the intrinsic elastic stiffness of a syntactic foam without unintentionally included voids.

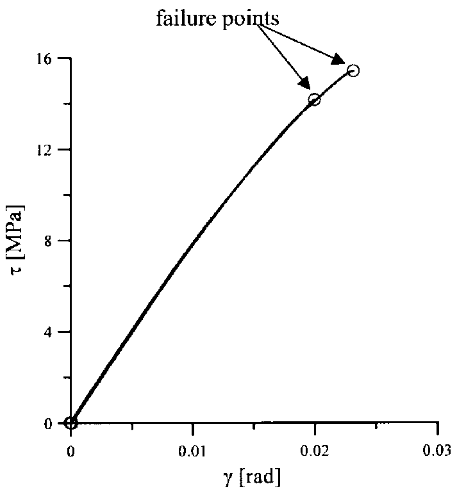

Fig. 3 Maximum shear stress-strain curves for the torsion tests on the syntactic foam

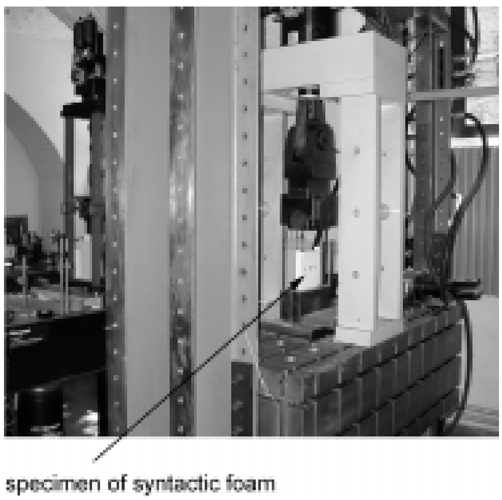

Fig. 4 Biaxial fatigue testing device used for the biaxial compression tests on the syntactic foam

3.4 Biaxial compression tests on the syntactic foam

The biaxial fatigue testing device (Fig. 4) was used for the biaxial compression tests**.** Owing to the lack of specific standards, squared panels were adopted, with dimensions based on the end-grips characteristics (Fig. 5a). Strains were measured by electric strain gauges directly glued onto the specimens. Tests were made under force control, considering three different radial paths in compression/compression: the ratio between horizontal to vertical force were equal to 1/3, 2/3 and 1/1. To compare the results with the compression tests on cylindrical specimens, a uniaxial compression test with ratio equal to 0/1 was also performed. Table 4 gives the failure stresses corresponding to the peak load. It can be noticed that the uniaxial compressive strength is practically identical to the one obtained for the cylindrical specimens of the second group.

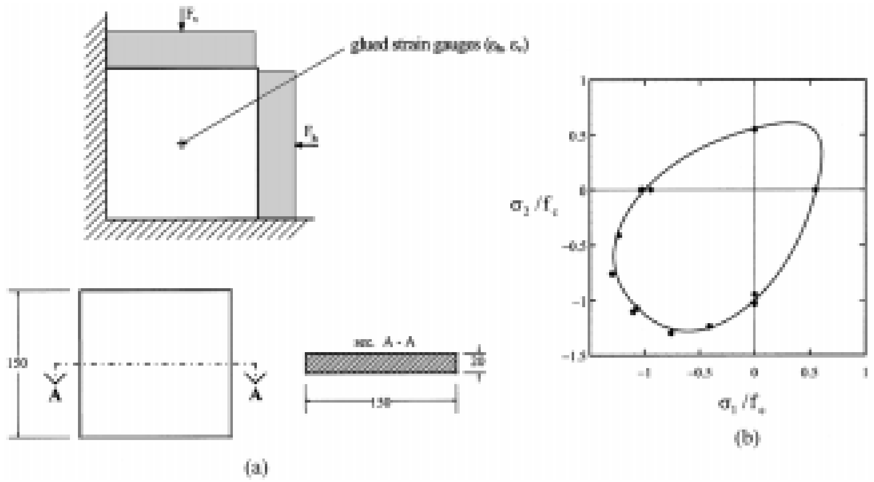

Fig. 5 Biaxial compression tests on the syntactic foam: (a) specimen geometry (dimensions in mm); (b) failure points and calibrated Drucker-Prager failure envelope in the principal stress plane

Table 4 Experimental data of biaxial compression tests on the syntactic foam manufactured by the producer: vertical and horizontal peak stresses at failure

F_h/F_v	σ_h (MPa)	σ_v (MPa)
0	0.00	27.60
1/3	11.70	35.12
2/3	21.57	36.90
1/1	31.33	31.33

Moreover, the strength under equi-biaxial compression (load ratio 1/1) is lower than the biaxial strengths obtained with load ratios 1/3 and 2/3. Fig. 5b represents the set of all failure points in the plane of principal stresses (with the symmetric points and the failure envelope calibrated with an elastic-plastic modified Drucker-Prager model, Rizzi *et al.* 2000). It can be observed that the egg-shaped failure locus is similar to biaxial failure domains observed for many frictional geomaterials. In all tests, failure was characterised by microsphere crushing on an horizontal layer near the upper vertical platen.

3.5 Three point bending tests on the syntactic foam

The three point bending tests on notched specimens were carried out on the Instron 8652 machine. The specimen dimensions were chosen according to the ASTM E 399 and are reported in Fig. 6a. Previous tests on a similar syntactic foam suggested to use specimens of the smallest-possible size, in order to avoid excessively brittle responses, while, on the other hand, sizes had also to be compatible with the requirements posed by the testing devices. The syntactic foam under testing turned out to be in practice more brittle than the previous one.

Four tests were made under vertical displacement control at a rate of 0.2 μm/s: the small specimen size did not allow to drive the tests under monotonic crack mouth opening, a provision which allows also to trace possible snap-back branches of the load vs. vertical displacement curves. These

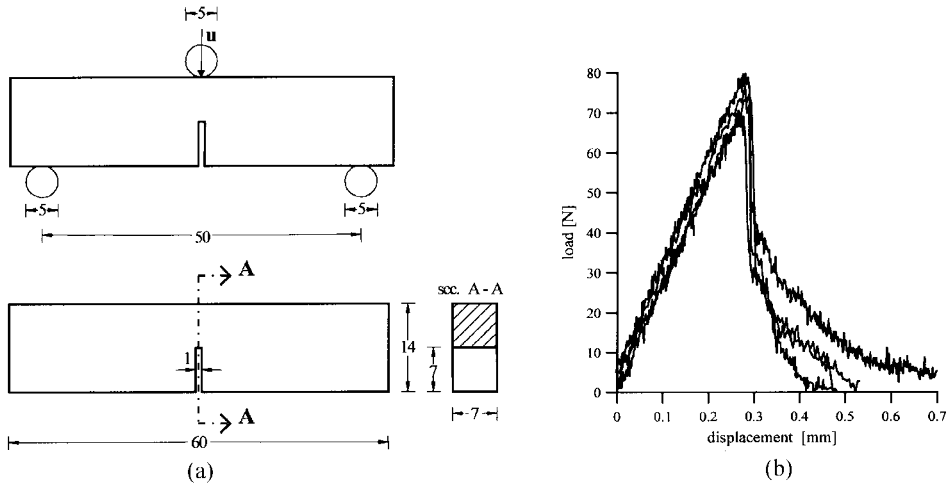

Fig. 6 Three Point Bending tests on notched syntactic foam specimens: (a) specimen geometry (dimensions in mm); (b) load-displacement curves

curves are reported in Fig. 6b: the behaviour is quasi-brittle with a practically-vertical load drop right after peak and a subsequent softening tail of residual strength. Failure is due to a crack that initiates and propagates vertically right above the sharp-edged notch.

4. Experimental tests on the extra-skins and assembled composite sandwich

The experimental tests performed on both extra-skins and assembled composite sandwich elements are now presented. The test features were chosen according to the ASTM standards for composite sandwiches. The sandwich specimens were obtained by cutting them out of three panels of composite sandwich provided directly by the manufacturer.

The first panel (total thickness 15 mm with a core of 9 mm) presented, even at eye-sight, one skin with a smoother surface and the other skin with the weft-warp structure of the ROVING 900™ tissue visible by the 10 mm edge periodic square cells. Also, the piles inside the core were inclined at about 45° owing to an incomplete stretching along the thickness direction. In the second and third panels the extra-skin structure was no more visible since it was covered by a layered epoxy resin. The core thickness was 10 mm, that is 1mm deeper, and correspondingly the sandwich composite was 16 mm thick. However, the piles were still inclined.

When cutting the specimens out of the panels, the preferential orientation in the sandwich plane due to the piles slope along the warp direction was taken into account: the specimens for edgewise compression and flatwise bending tests were divided into two groups, the first with the longer dimension along the weft direction, the second with the longer dimension along the warp direction.

4.1 Uniaxial tension tests on the sandwich extra-skins

These tests were done in order to quantify the elastic properties of the extra-skins. The specimens were cut along both weft and warp directions of the extra-skins. The specimen ends were reinforced by gluing on both sides of the extra-skin two additional resin-glass tabs (Fig. 7a). These tabs may however induce local stiffening and lead to a premature breaking of the specimen near the grip ends, as sometimes recorded in our experiments. Seven tests were carried out for each direction under displacement control by imposing a constant cross-head velocity of 1 mm/min. Strains were measured by axial strain gauges glued onto the specimen.

Table 5 reports the average values of the experimental data, whereas Fig. 7b shows the stress-strain curves along the warp and weft directions for one of the tests. The responses are again rather brittle with a stiffness which is about the same for the two cases, while the strength is significantly lower (about one half) for the weft direction. The specimens response is non-linear: since the available stress-carrying cross section decreases due to the progressive fracture of fibres, the nominal stress grows non-proportionally.

4.2 Flatwise compression on the sandwich panels

Flatwise compression tests allow the evaluation of strength and stiffness of the sandwich core under compression. Comparing the results with the experimental data obtained from the uniaxial compression tests on the plain syntactic foam, it is possible to enquire the effects of the piles on the global mechanical properties of the sandwich core.

Specimen shape and size were determined according to the ASTM C 365: squared panels with sides of 25 mm were adopted (see Fig. 8a). Following the method recommended by the ASTM, the displacements were measured by using four LVDT clamped to the loading platen (Fig. 8b). Owing

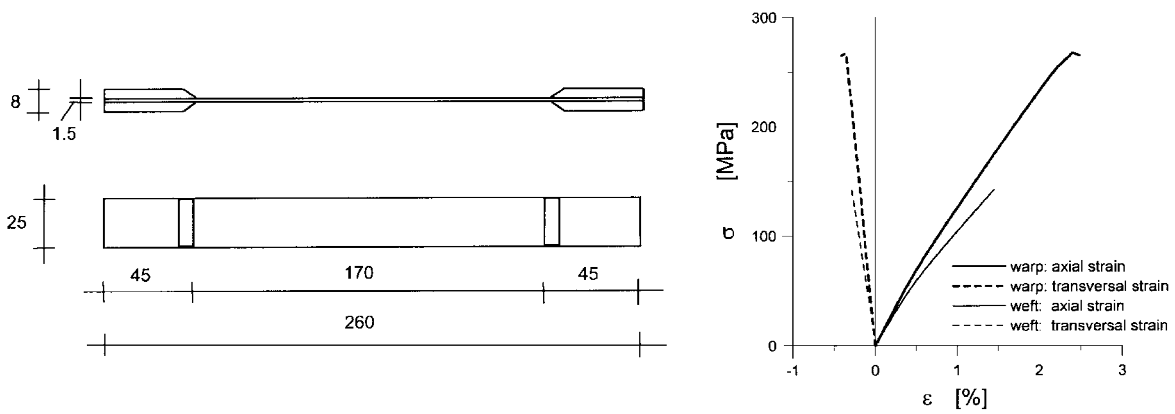

(a) (b)

Fig. 7 Uniaxial tension tests on the GFRP skins: (a) specimen geometry (dimensions in mm); (b) stress-strain curves

Table 5 Experimental data of uniaxial tension tests on the GFRP extra-skins along both warp and weft directions

	E (MPa)	ν	σ_{peak} (MPa)	ε_{peak} (%)
warp	18100	0.13	210	2
weft	14200	0.14	175	2

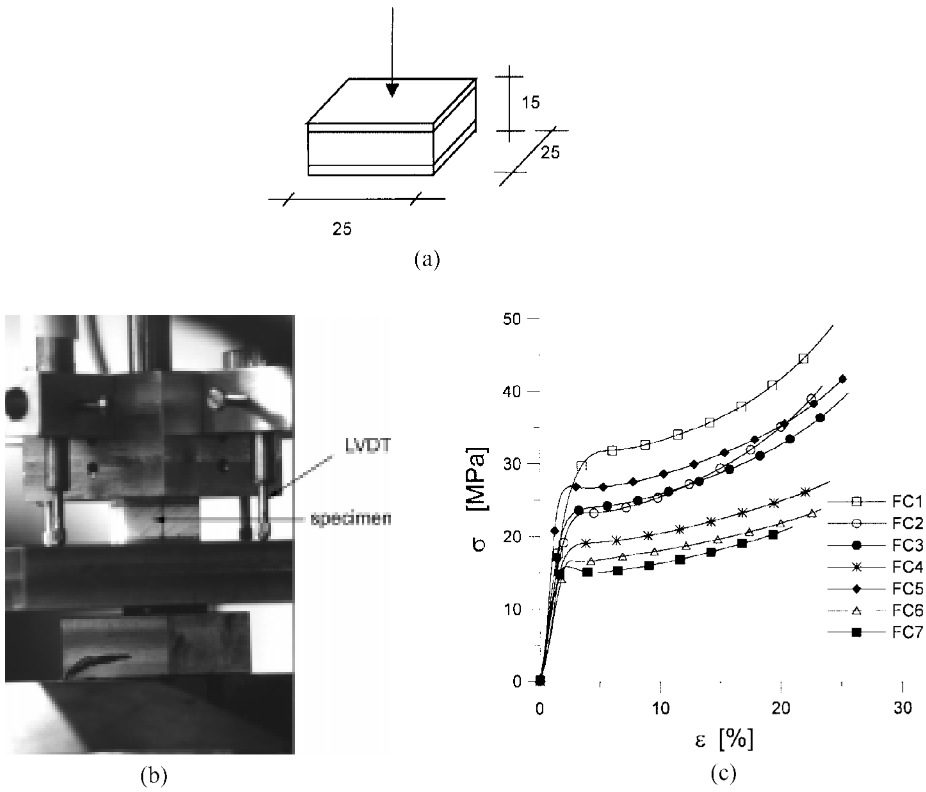

Fig. 8 Flatwise compression tests on the sandwich: (a) specimen geometry (dimensions in mm); (b) experimental setup; (c) stress-strain curves

to the irregularities of the sandwich thickness, the opposite faces were not perfectly parallel. Hence, the reference values of displacement and load corresponded to a preloading of 100 N. The tests were driven under displacement control at a constant cross-head velocity of 0.5 mm/min.

Table 6 gathers the experimental results obtained from the seven carried out tests. The considerable data scattering, especially in terms of stiffness, is due to the geometric non-homogeneity of the specimens. Indeed, these specimens were cut from different zones of the same panel which possessed different densities due to an imperfect production technology. In Table 6 the value of stress σ_{max} corresponding to a 0.2% strain is shown, as suggested by the norm. The values of elastic stiffness are computed with reference to the core strain only, i.e. Young's modulus E is equal to the initial stiffness taken from the load-displacement curve, divided by the initial cross section and multiplied by the core thickness. The first two columns of Table 6 contain weight and volume of each specimen, respectively, which are used to compute the specific weight. Table 6 reports also the void percentage (v%) as estimated from the nominal and real specific weights of the specimens (*nsw* and *rsw*, respectively) by using the following expression: $v\% = 1.-(rsw/nsw)\ 100$. The nominal specific weight of each specimen is computed by multiplying the density of each component for its thickness: the sum of the values obtained is then multiplied by the area and divided by the total volume.

Fig. 8c shows the stress-strain curves of the different specimens; by comparing Fig. 8c and the data in Table 6 it can be noticed that the strength and stiffness decrease with voids increase.

Table 6 Experimental data of flatwise compression tests on the composite sandwich

Test number	Weight (g_f)	Volume (cm^3)	Specific weight (g_f/cm^3)	Voids %	E (MPa)	σ_{max} (MPa)
FC1	9.80	9.83	1.00	21.6	1148	23
FC2	10.01	10.38	0.96	22.6	1054	21
FC3	9.39	10.54	0.89	25.7	1290	21
FC4	8.29	9.83	0.84	31.2	1053	17
FC5	8.86	10.02	0.88	26.3	1765	26
FC6	8.21	9.87	0.83	31.9	845	16
FC7	8.40	10.00	0.84	30.0	687	16

Possible deviations from this behaviour are due to the inhomogeneous void distribution: a local macrovoid makes a specimen weaker than one with widespread microvoids. In each stress-strain curve the initial linear behaviour is followed by a knee after which the stress grows slowly. Such locking response is induced by the containment effect due to the skins and to the interaction between piles and syntactic foam. The containment and shearing associated to the relative sliding of the upper and lower faces induced by the piles inclination produces into the specimen a true triaxial stress state. The pressure-dilatation curve of a Cenosphere syntactic foam (Luxmoore and Owen 1982) is qualitatively similar to the locking behaviour displayed by the sandwich core. Finally, three cyclic tests with unloading right after the linear range have shown an hysteretic behaviour with absence of cyclic hardening.

4.3 Flatwise tension on sandwich panels

Sandwich structures are normally subjected to flatwise or edgewise compression and bending. However, flatwise tension tests allow to measure the skin-core interface strength, which is a critical point in the sandwich structure: if delamination phenomena develop in this zone, core and skin are no more able to transfer stresses and consequently the structure functionality vanishes.

These tests must comply with the ASTM C 297-94. Same as for the flatwise compression tests, the specimens were parallelepipeds with a square base of 625 mm^2 (see Fig. 9a), namely the lower bound prescribed by the norm. Ten tests were carried out under displacement control with a displacement rate of 0.5 mm/min. Traction was imposed perpendicularly to the lamination plane through two stiff loading blocks glued to the skins. A convenient end-grip was fixed at each block through an horizontal pin: to assure the load alignment the two end-grips were placed at 90° with respect to each other (Fig. 9b).

To allow testing, the adhesive must possess a tensile strength higher than that of the specimen. Accordingly, a bicomponent epoxy glue with maximum strength of 3000 MPa was chosen. Since the goal of these tests was only that of determining the tensile strength of the skin/core interface, measure instruments were not applied onto the specimens.

Only two of the tests failed due to the loss of adhesion, probably owing to the improper cleaning of the glued surfaces, while for all the other tests the failure happened for separation between extra-skins and skins. Two sets of specimens were considered, five tests were carried out for each group. The first gave an average value of the maximum stress equal to 0.62 MPa, while the second gave 5.85 MPa. This sensible difference is probably due to the resin used for impregnating the sandwich-fabric bond and the extra-skins tissues: in the first case two different resins were used for the two

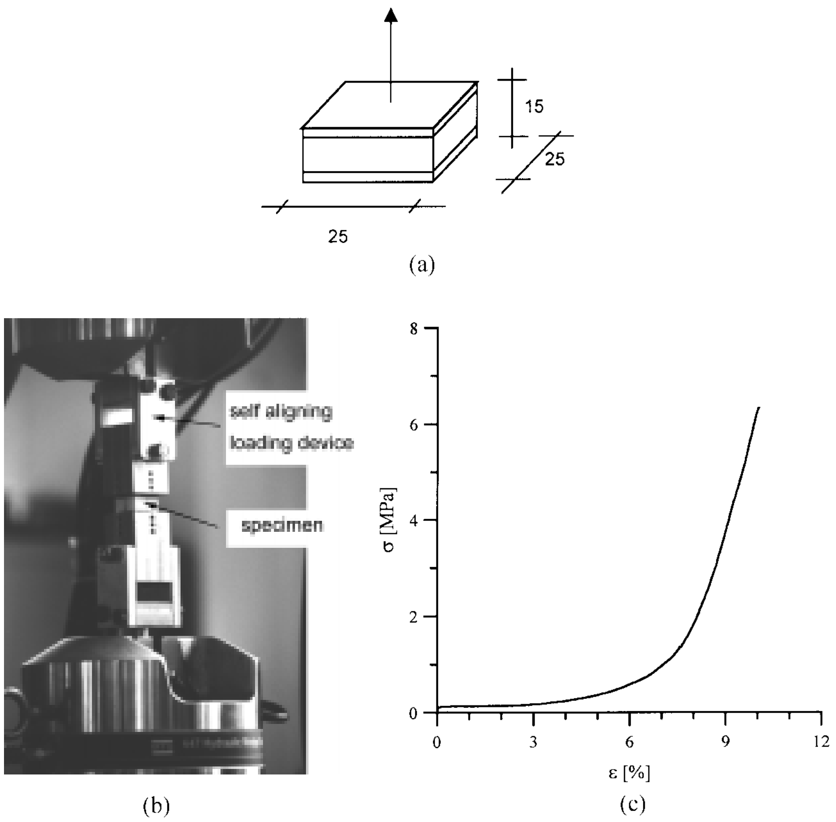

Fig. 9 Flatwise tension tests on the sandwich: (a) specimen geometry (dimensions in mm); (b) experimental setup; (c) stress-strain curve

skins (epoxy for sandwich-fabric bond and polyester for extra-skins), whereas the skins of the second set were treated with the same epoxy resin that was used for the other sandwich components.

Fig. 9c shows the stress-strain curve of one of the tests of the second set: the initial non-linear behaviour with slow stress increase is due to the arrangements of the loading device. Rupture is perfectly brittle. The weakness of the interface between sandwich-fabric bond and extra-skins shows clearly that the simple superposition of laminates cannot assure enough strength for tensile loading perpendicular to the sandwich plane. Accordingly, it would be more appropriate to strengthen the sandwich-fabric facings directly by weaving additional skins interconnected with the piles.

4.4 Edgewise compression on sandwich panels

Edgewise compression tests were performed following the ASTM C 364 and allowed to account for the bearing capacity of sandwich panels. The collapse can be due to global buckling or local instability. For example a particularly deformable core may induce local skins instability (wrinkling); however, since the core must be sufficiently stiff in the flatwise direction (to maintain the fixed distance between the skins) this kind of collapse seldom appears. On the contrary, failures due to global buckling of the whole specimen are more frequent, which can induce separation between skins and core, or skins crimping at the extremities.

To avoid loading eccentricity and lateral confinement, a good alignment of loading devices and superficial treatment of the specimen end sections are required. Centrality and perpendicularity of the loading direction were verified by measuring strains during the initial test phase. Strain gauges were applied on the two opposite skins: the measured strains were equal within a tolerance up to 5%. The specimen size was 90 mm in the direction parallel to the loading and 50 mm in the direction orthogonal to it (see Fig. 10a).

The ends of the specimens were packed with two brass clamps made by two rectangular bars held tightly together through pushing screws. In this way the delamination for loss of adherence between skin and core near the contact zones was prevented.

Eight tests were carried out for each direction under displacement control at a constant displacement rate of 0.5 mm/min. The specimens loaded in the direction of piles sloping (weft direction) gave an average value of failure stress and stiffness equal to 61 MPa and 6941 MPa, respectively. On the contrary, for the specimen loaded in the orthogonal (warp) direction, these values lowered to 57 MPa and 5889 MPa, respectively.

Fig. 10b represents a typical stress-strain curve. After the initial settlement the behaviour is linear until the first rupture occurs (usually in the skins). Then, the damaged structure shows a fast separation between skins and core due to further cracking of the extra-skins. The sandwich failure is never due to core subsiding: this fact confirms the efficiency of transverse junction due to the piles and the rather poor adhesion between sandwich-fabric bond and extra-skins.

Usually, the final failure is due to skins instability (see Fig. 11): core and ROVIMAT possess different compression stiffness and consequently sustain different loading, higher in the ROVIMAT. Moreover, while piles oppose the transverse strains of the core, the weakness of the interface between extra-skins and sandwich-fabric bond and the thinness of the two strata induce an independent flexural behaviour. Wrinkling phenomena are not present since the skin-core adhesion is not so strong to allow load transfer. After separation, the skins break due to compression instability: cracks are inclined into the thickness at about 45°.

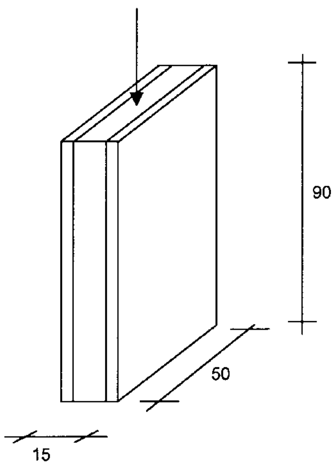

(a)

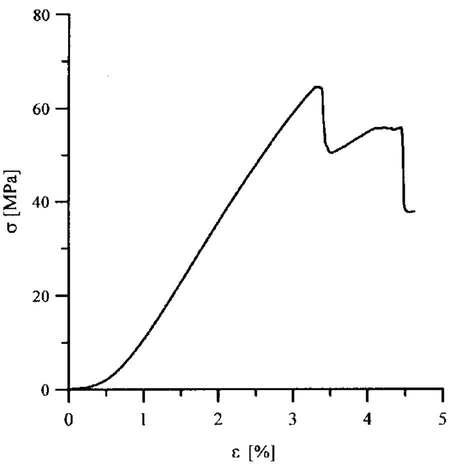

(b)

Fig. 10 Edgewise compression tests on the sandwich: (a) specimen geometry (dimensions in mm); (b) stress-strain curve

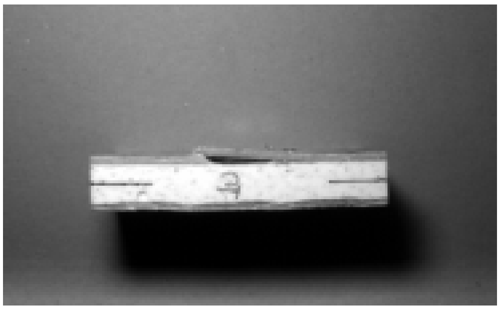

Fig. 11 Edgewise compression tests on the sandwich: typical failure mode with skin delamination and rupture

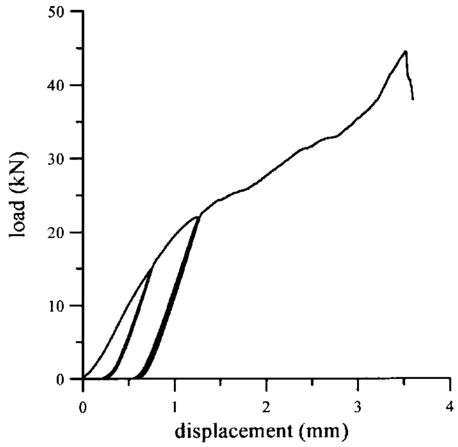

Fig. 12 Edgewise compression tests on the sandwich: load-displacement curve of a test with loading/ unloading cycles

Finally, three tests were performed by considering three unloading/reloading cycles: the load-displacement curve follows the same path during unloading and reloading; after reloading it reaches the original point and then follows the original trend (see Fig. 12).

4.5 Three and four point bending tests on sandwich panels

Flatwise bending tests give several information on the sandwich behaviour. In particular they allow evaluation of the shear strength of the core, the in-plane strength of the skins and the strength of the skins-core interface.

Tests were performed referring to the ASTM C 393. The norm gives indications on the specimen geometry, depending on the purpose of the test. Short specimens must be used to assess the core shear properties: in this way the stress states in the skins due to the bending moments are lower than the limit values. On the contrary, traction and compression strengths of the skins can be determined by testing long specimens. Since in the present study the skins properties were investigated separately (Section 4.1), the tests were performed with short specimens in order to obtain the shear characteristics of the core and the global bending behaviour.

The bending stiffness and shear modulus are determined by comparing displacements and loads of three and four point bending tests on the same specimen. Obviously, the loading imposed during the first test must induce stresses below the elastic limit.

Each specimen, 110 mm long and 30 mm wide, had an average thickness of 15 mm. It was loaded by a knife (with a diameter of 8 mm) for the three point bending tests and by two rolls 20 mm distant (with diameter also equal to 8 mm) in the case of the four point bending tests. The specimens were supported by two cylinders with a diameter of 24 mm and span of 60 mm (see Figs. 13a, b).

To compute the shear modulus G of the core, two methods are proposed by the ASTM standard. In the first method, the shear contribution to the vertical displacement at mid-span section is obtained by subtracting the pure elastic bending part from the experimental data Δ measured at that point. Indeed, in the elastic range:

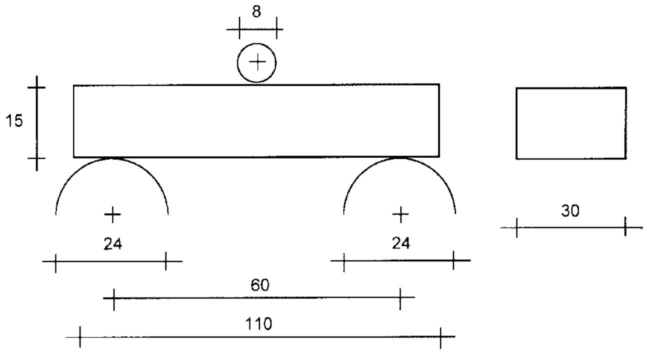

(a)

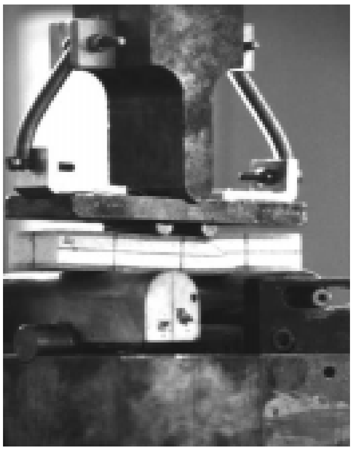

(b)

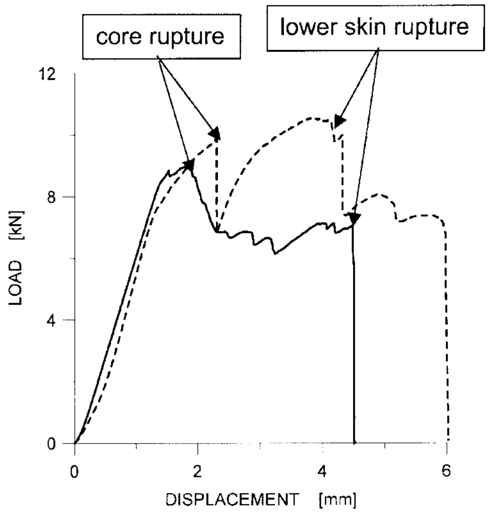

(c)

Fig. 13 Three point bending tests on the sandwich: (a) specimen geometry; (b) experimental setup; (c) load-displacement curves

$$\Delta = \frac{PL^3}{48K_B} + \frac{PL}{4K_S} \tag{1}$$

with

$$K_S = \frac{Gb(d+c)^2}{4c} \tag{2}$$

where $d=(c+t)$, c is the core thickness and t the thickness of one skin. K_B represents the bending stiffness, K_S the shear stiffness of the sandwich, P the applied load, L the distance between the supports, and b the specimen width. Then, knowing the bending stiffness and obviously the experimental value Δ, Eq. (1) allows the direct evaluation of the shear modulus G.

The second method proposed by the ASTM for evaluating the shear modulus of the core is based on the comparison between experimental data of three and four point bending tests carried out on the same specimen. The expression of G in this case is

$$G = \frac{P_1 L_1 c[(8L_1^2/11L_2^2) - 1]}{\Delta_1 b(d+c)^2[(16P_1 L_1^3 \Delta_2/11P_2 L_2^3 \Delta_1) - 1]} \tag{3}$$

where the quantities with subscript 1 (2) are relevant to three (four) point bending tests.

To compute the bending stiffness K_B, the standard proposes two methods. In the first one, this mechanical characteristic is also obtained by comparing the results of three and four point bending tests:

$$K_B = \frac{P_1 L_1^3[1 - 11L_2^2/8L_1^2]}{48\Delta_1[1 - 2P_1 L_1 \Delta_2/P_2 L_2 \Delta_1]} \tag{4}$$

The second method is purely analytical. K_B is evaluated by using the following expression:

$$K_B = \frac{Eb(d^3 - c^3)}{12} \tag{5}$$

where E is the elastic modulus of the skin only. Actually, a complete expression of the bending stiffness accounting correctly for the skins and core stiffness should be

$$K_B = E_S \frac{bt^3}{6} + E_S \frac{btd^2}{2} + E_C \frac{bc^3}{12} \tag{6}$$

where E_S and E_C are Young's moduli of skins and core, respectively. Although skins are thick and Young's modulus of the core is greater than that of the skins, the first and third term of expression (6) can be neglected in practice. The difference between values of K_B obtained from Eqs. (5) and (6) is about 2.5%. This difference does not affect substantially the value of the shear modulus G.

Table 7 shows first the values of the shear modulus G and of the bending stiffness K_B derived from Eqs. (1) and (5) and then the values obtained by solving together Eqs. (3) and (4). It is worth-mentioning that with this second method the bending stiffness is not a constant along the specimen since it depends on the real distribution of defects. Moreover, the shear modulus of core depends on the piles inclination (along the 110 mm or the 30 mm side): G is greater for the specimens with piles inclined along the longer side.

To obtain the shear strength of the core, eight three and four point bending tests were performed until failure. Fig. 13c shows the load vs. vertical displacement curves for two specimens subjected to the three point bending test. The first rupture is always localised into the core, while final failure is due to a macrocrack connecting the loading roll with the support roll. In the specimens with piles oriented along the 110 mm side, the macrocrack is parallel to the same piles (Fig. 14). In several four point bending tests on specimens with piles sloping along the short side, two symmetrical macrocracks grow simultaneously, always connecting the loading and support roll (Fig. 15). It is

Table 7 Experimental data of three and four point bending tests on the composite sandwich: estimated shear modulus of the core G and bending stiffness of the sandwich K_B

	G (Eq. 1) (MPa)	K_B (Eq. 5) (N mm^2)	G (Eqs. 3,4) (MPa)	K_B (Eqs. 3,4) (N mm^2)
Piles inclined along the specimen length	229	10781924	271	11225439
Piles inclined along the specimen width	167	10781924	141	11318564

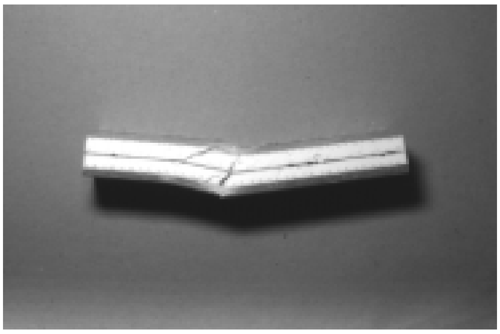

Fig. 14 Three point bending tests on the sandwich: typical unsymmetric core failure with cracks parallel to the inclined piles

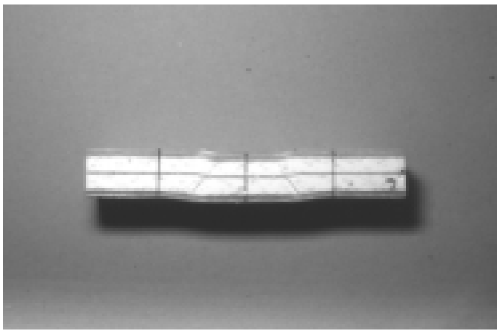

Fig. 15 Four point bending tests on the sandwich: typical symmetric core failure

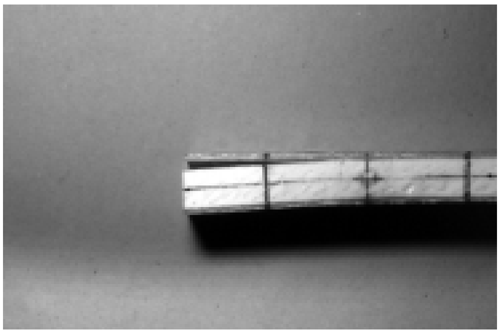

Fig. 16 Four point bending tests on the sandwich: typical failure mode with extra-skin delamination

important to note that in two cases of the four point bending tests, failure has been due to separation between extra-skins and core (Fig. 16). In other tests, analogously to the tension flatwise tests, separation occurred between skins and extra-skins: this fact confirms the efficiency of the piles and the inadequacy of the simple superposition of the extra-skins.

5. Conclusions

This paper presented the main results of an experimental campaign on the mechanical behaviour of a light composite sandwich. Tests were performed on the individual sandwich components (syntactic foam and skins) and on the assembled sandwich elements. In view of a first characterisation of the mechanical performances, the scheduled number of tests did not allow in practice a statistical treatment of the results scattering. In spite of this limitation, the tests performed allowed to quantify the salient mechanical features of the material under study.

The innovation of the composite sandwich technology analysed in this work is represented by the presence of a true three-dimensional fabric structure embedded inside the sandwich, which is conceived to avoid the serious problem of delamination between skins and core. The effectiveness of such technology is validated by the experimental results as obtained here. However, in several tests the delamination failure moved to the now-weaker interface between skins and extra-skins, which are simply superimposed. This new weak point of the composite sandwich, as shown by the present tests, should be stiffened in an appropriate way, for example, by sewing together extra-skins and skins.

The experimental tests have also shown a significant anisotropic behaviour, which depends on the loading direction with respect to piles slope (which are inclined due to an incorrect manufacturing procedure). For example, in the edgewise compression tests, the stiffness and strength of specimens loaded in the weft direction (piles sloping along the loading direction) are 18% and 8.5% greater than the values of the specimens loaded in the warp direction. In fact, in the first kind of specimens the piles are subjected to tensile stress and, due to their high stiffness, they constrain the specimen's strain in the transverse direction. Analogous stiffening is present in the specimens subjected to flatwise bending (three and four point bending tests). Consequently, a proper manufacturing procedure with complete piles stretching is strongly recommended to avoid unwanted anisotropic behaviour of the core in the middle plane of the sandwich. More generally, accurate manufacturing procedures are particularly recommended for this new composite technology, to avoid that part or all the benefits brought about at design stage may be lost in practice.

The piles allow not only a better adhesion between skins and core, but also influence the properties of the core. On one side, the flatwise compression tests on the sandwich show that the sandwich stiffness is about 35% lower than that of the syntactic foam (see Tables 1 and 6); also, the sandwich strength is significantly lower than that of the syntactic foam (19 MPa vs. 30 MPa, respectively). However, the core with embedded piles shows further deformation resources over the elastic limit, since the sandwich displays a considerable ductile behaviour, whereas the elastic limit of the syntactic foam coincides practically with its failure point.

As a last comment, although the tested sandwich panels were not of the preferred geometry, the validity of the innovative skin-core interconnection provided by the piles was proved by the present tests independently of the vice of the piles inclination. Unfortunately, comparison tests with preferred sandwich geometries could not be performed since proper specimens were not available. Despite this intrinsic limitation, the results presented here include not only the overall performance of the sandwich, but also the mechanical response of the various sandwich components, chiefly the syntactic foam used to fill the sandwich core and the extra-skins that are laminated on the external facings of the sandwich. Most of these results are totally independent of the incomplete piles stretching.

Finally, further tests should be made to broaden the mechanical investigation on this sandwich composite. Firstly, the same tests should be repeated in order to gather a more complete and reliable set of mechanical results allowing also statistical treatments. Then, other significant aspects of the mechanical behaviour should be considered in view of the many possible uses of the composite sandwich, among them: triaxial behaviour, fatigue and creep phenomena, and variation of mechanical properties with temperature.

Acknowledgements

The present paper originated from a research project between Intermarine S.p.A. and Politecnico di Milano headed by Prof. Giulio Maier at the Dept. of Structural Engineering. At the time the research was performed and the author E.R. was an employee of Politecnico di Milano. The authors wish to thank Intermarine S.p.A. for providing reference material on composites for naval engineering applications and for granting permission to publish the present results. We are grateful to Prof. Giulio Maier for involving us into this research topic and for fruitful discussions on selected related subjects. We acknowledge the contributions of our former students Luca Lobaccaro, Ilaria Schiavi and Mara Savioli who were involved in the present research during the preparation of their Laurea thesis.

References

Allen, H.G. (1969), *Analysis and Design of Structural Sandwich Panels*, Pergamon Press, Oxford.

ASTM C 297 (1999), *Standard Test Method for Flatwise Tensile Strength of Sandwich Constructions*, Annual Book of ASTM 1999, Vol. 15.03, *Space simulation; Aerospace and Aircraft ; High Modulus Fibers and Composites*, ASTM, New York.

ASTM C 364 (1999), *Standard Test Method for Edgewise Compressive Strength of Sandwich Constructions*, Annual Book of ASTM 1999, Vol. 15.03, *Space simulation; Aerospace and Aircraft; High Modulus Fibers and Composites*, ASTM, New York.

ASTM C 365 (1999), *Standard Test Method for Flatwise Compressive Properties of Sandwich Cores*, Annual Book of ASTM 1999, Vol. 15.03, *Space simulation; Aerospace and Aircraft; High Modulus Fibers and Composites*, ASTM, New York.

ASTM C 393 (1999), *Standard Test Method for Flexural Properties of Sandwich Constructions,* Annual Book of ASTM 1999, Vol. 15.03, *Space simulation; Aerospace and Aircraft; High Modulus Fibers and Composites*, ASTM, New York.

ASTM D 638 (1999), *Standard Test Method for Tensile Properties of Plastics Materials,* Annual Book of ASTM 1999, Vol. 8.01, Plastics, ASTM, New York.

ASTM D 695 (1999), *Standard Test Method for Compressive Properties of Rigid Plastics,* Annual Book of ASTM 1999, Vol. 8.01, Plastics, ASTM, New York.

ASTM E 399 (1999), *Standard Test Method for Plane-Strain Fracture Toughness of Metallic Materials,* Annual Book of ASTM 1999, Vol. 3.03, Metals tests methods and analytical procedures, ASTM, New York.

Corigliano, A., Rizzi, E., and Papa, E. (2000), "Experimental characterization and numerical simulations of a syntactic foam/glass fibre composite sandwich", *Composites Science and Technology*, **60**(11), 2169-2180.

Hull, D., and Clyne, T.W. (1996), *An Introduction to Composite Materials*, Cambridge University Press.

Kuenzi, E.W. (1965), *Minimum Weight Structural Sandwich,* U.S. Forest Service Res. Note FPL-086.

Luxmoore, A.R., and Owen, D.R.J. (1982), "Syntactic foam", *Mechanics of Cellular Plastics*, N.C. Hilyard Ed., Applied Science Publishers LTD, London.

Palumbo, M., Donzella, G., Tempesti, E., and Ferruti, P. (1996), "On the compressive elasticity of epoxy resins filled with hollow glass microspheres", *J. Applied Polymer Science*, **60**, 47-53.

Palumbo, M., and Tempesti, E. (1997), "The effect of particle-matrix interfacial conditions on the compressive elasticity of epoxy resins filled with untreated hollow glass microspheres", *Polymers & Polymer Composites*, **5**(3), 217-221.

Palumbo, M., and Tempesti, E. (1998), "On the nodular morphology and mechanical behaviour of a syntactic foam cured in thermal and microwave fields", *Acta Polymerica*, **49**, 482-486.

Papa, E., and Nappi, A. (1995) "A test rig for the application of biaxial cyclic loads to structural models", *Mater. and Struct.*, **28**, 299-307.

Plantema, F.J. (1966), *Sandwich Construction*, Wiley & Sons, New York.

Rizzi, E., Papa, E., and Corigliano, A. (2000), "Mechanical behaviour of a syntactic foam: experiments and modeling", *Int. J. Solids and Structures*, **37**(40), 5773-5794.

Smith, C.S. (1990), *Design of Marine Structures in Composite Materials,* Elsevier Applied Science, London-New York.

van Vuure, A.W. (1997), "Composite panels based on woven sandwich fabric preforms", PhD Thesis, Katholieke Universiteit Leuven.

van Vuure, A.W., Pflug, J., Ivens, J.A., and Verpoest, I. (2000), "Modelling the core properties of composite panels based on woven sandwich-fabric preforms", *Compos. Sci. and Technol.*, **60**, 1263-1276.